

A COMPREHENSIVE EVALUATION OF THE ETA-CMAQ FORECAST MODEL PERFORMANCE FOR O₃, ITS RELATED PRECURSORS, AND METEOROLOGICAL PARAMETERS DURING THE 2004 ICARTT STUDY

Shaocai Yu^{+\$}, Rohit Mathur⁺, Kenneth Schere⁺, Daiwen Kang^{+\$},
Brian Eder⁺, Jonathan Pleim⁺, and Tanya Otte⁺

Atmospheric Sciences Modeling Division, Air Resources Laboratory,
National Oceanic and Atmospheric Administration, RTP, NC 27711

⁺On assignment to National Exposure Research Laboratory,
U.S. Environmental Protection Agency, Research Triangle Park, NC 27711

^{\$} On assignment from Science and Technology Corporation,
10 Basil Sawyer Drive, Hampton, VA 23666-1393

1. INTRODUCTION

Ozone (O₃), a secondary pollutant, can adversely affect human and ecosystem health, and is a major concern in the U.S. It is desirable for local air quality agencies to accurately forecast ozone concentrations to alert the public of the onset, severity and duration of unhealthy air and to encourage people to voluntarily reduce emissions-producing activities. In this study the performance of the Eta-CMAQ forecast model is evaluated against extensive measurements collected during the 2004 International Consortium for Atmospheric Research on Transport and Transformation (ICARTT) field experiment.

2. DESCRIPTION OF THE ETA-CMAQ FORECAST MODEL SUITE AND OBSERVATIONAL DATABASE

The Eta-CMAQ air quality forecasting system (Otte et al., 2005), created by linking the Eta model (Rogers et al., 1996) and the U.S. EPA's CMAQ Modeling System (Byun and Ching, 1999), is deployed over the domain of the eastern U.S. during summer 2004. The domain has a horizontal grid resolution of 12 km. Twenty-two layers of variable thickness set on a sigma-type coordinate are used to resolve the vertical extent from the surface to 100 hPa. The primary Eta-CMAQ model forecast for next-day's surface-layer O₃ is based on the current day's 12 UTC Eta cycle. The target forecast period is local midnight through local

midnight (04 UTC to 03 UTC). The emissions are projected to 2004 from the 2001 U.S. EPA national emission inventory (Pouliot, 2005). The Carbon Bond chemical mechanism (version 4.2) is used to represent reaction pathways.

The hourly O₃ data at 614 sites in the eastern U.S. are available from the U.S. EPA's Air Quality System (AQS) network (Figure 1). Four Atmospheric Investigation, Regional Modeling, Analysis, and Prediction (AIRMAP) sites provided continuous measurements of O₃ and related photochemical species as well as meteorological parameters during the study; the sites include Castle Springs (CS), Isle of Shoals (IS), Mount Washington Observatory (MWO), and Thompson Farm (TF). From July 1 to August 15, 2004, measurements of vertical profiles of O₃, its related chemical species (CO, NO, NO₂, H₂O₂, CH₂O, HNO₃, SO₂, PAN, isoprene, toluene), and meteorological parameters (liquid water content, water vapor, temperature, wind speed and direction and pressure) were carried out by extensively instrumented aircraft (NOAA P-3 and NASA DC-8) and Lidar deployed as part of the 2004 ICARTT field experiment. The model performance from July 1 to August 15, 2004, based on the 12 UTC run for the target forecast period, is examined in this study.

3. RESULTS AND DISCUSSION

3.1 Spatial and temporal evaluation over the eastern U.S. domain at the AIRNOW sites

Figure 1 shows that the model reproduced the majority (73.1%) of observed peak 8-hr O₃

* **Corresponding author address:** Shaocai Yu, E-243-01, NERL, U.S. EPA, RTP, NC 27711; e-mail: yu.shaocai@epa.gov

concentrations within a factor of 1.5. The model captured the daily variation of observed peak 8-hr O₃ concentrations very well. The scatter plot shows that the model generally over predicted the observations in the low O₃ concentration ranges, in part, due to the assumed high background O₃ levels specified in these simulations. Spatially, the model performed better over the western part than eastern coastal part of the domain. The largest over prediction of the observed peak 8-hr O₃ concentrations existed across the northeast. The recommended performance criteria for O₃ by the U.S. EPA (1991) are: mean normalized bias ± 5 to $\pm 15\%$; mean normalized gross error 30% to 35%; unpaired peak prediction accuracy: ± 15 to $\pm 20\%$. The domain mean values of NMB (Normalized Mean Bias) and NME (Normalized Mean Error) during the ICARTT period for maximum 8-hr O₃ are 22.6% and 28.8%, respectively, slightly higher than the performance criteria for the unpaired peak O₃. The model had the best performance on August 8 (NMB=1.9%, correlation coefficient (r)=0.73) and the worst performance on August 12 (NMB=42.4%, r=0.47). A close inspection of the synoptic-scale meteorological conditions reveals that on August 8, the majority of the domain was dominated by clear sky with partial cloudiness only across the Florida under the high pressure, while on August 12, an active cold front stretched from the north to south accompanied by convective cloud cover and precipitation over the domain under the low pressure. As shown by the subsequent diagnostic analysis (Mathur et al., 2004), the significant overprediction in areas of cloud cover is mainly caused by the unrealistic transport of excessive amount of the high O₃ concentrations near the tropopause to the ground associated with downward entrainment in CMAQ's convective cloud scheme.

3.2 Evaluation of vertical profiles for O₃, its related species and meteorological parameters

Comparisons of modeled and aircraft- and lidar-based observed vertical profiles provide an assessment for the ability of the model to simulate the vertical structure of air pollutants and meteorological fields. Following Mathur et al. (2005), modeled results were extracted by "flying" the aircraft through the 3-D modeling domain for each flight; the spatial locations of the aircraft were mapped to the model grid, whereas hourly resolved model outputs were linearly interpolated to the corresponding observational times. The

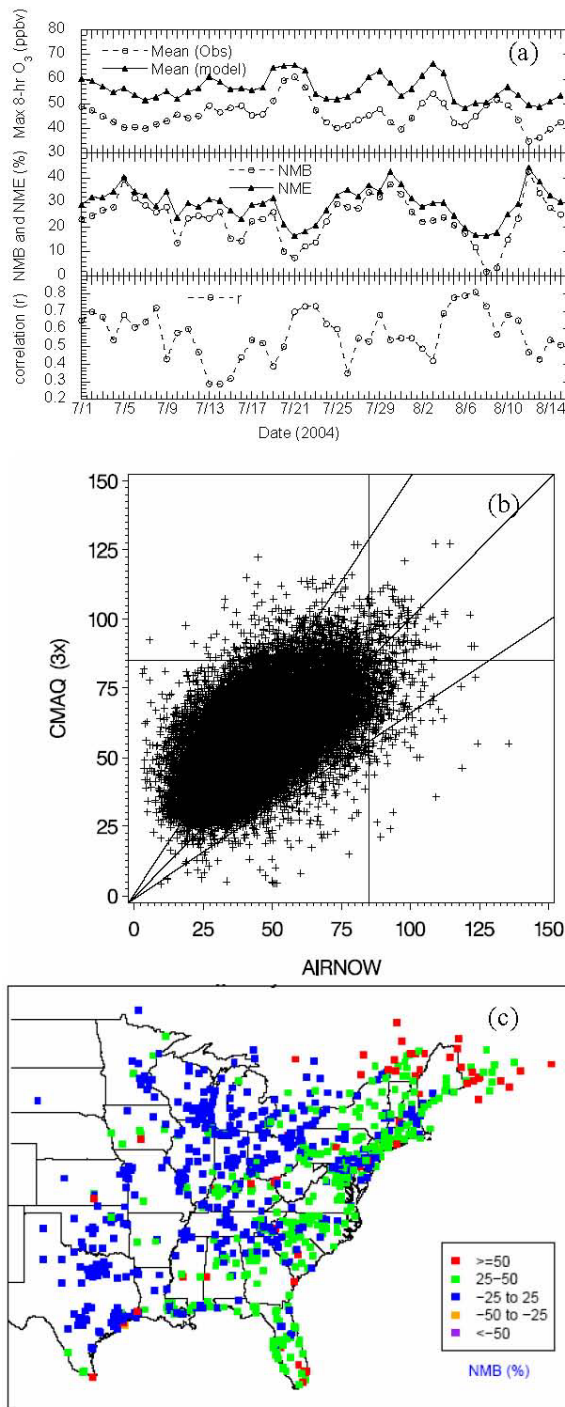


Fig. 1. Comparison of the modeled and observed peak 8-hr O₃ concentrations at the AIRNow monitoring sites (a) daily variation of mean, NME, NMB and correction (r), (b) scatter plot (ppbv) (The 1:1, 1.5:1 and 1:1.5 lines are shown for reference), and (c) spatial distribution of NMB during July 1 and August 15, 2004.

Tracks of aircraft show that measurements onboard the P-3 cover a regional area over the northeast around New York and Boston, whereas the DC-8 aircraft covers a broader regional area over the eastern U.S. All DC-8 measurements were conducted in the daytime (~7:00 to ~19:00 EST), and P-3 also conducted most of measurements at the daytime except 7/11, 7/31, 8/3, 8/7 and 8/9 in which the P-3 measurements were conducted in the nighttime (~20:00 to ~6:00 EST). In order to compare the modeled and observed vertical profiles, the observed and modeled data were grouped according to the model layer for each day and each flight, and then the layer mean values for each parameter were calculated. Thus, these vertical profiles may be regarded as representing the mean conditions along the flight track for each day. Figure 2 presents an example for modeled and observed vertical profiles for O₃ from the P-3, DC-8 and lidar measurements. It shows that while the model generally reproduced the observed O₃ vertical structure most of time, it tended to over predict in the upper layers. The model predicted more uniform vertical O₃ profiles than the observations and the over predictions increase with altitude based on the lidar results due to the coarse resolution for the vertical structure in the model.

The model's ability to simulate the vertical profiles for other parameters (CO, HNO₃, SO₂, NO, HCHO) measured by the P-3 and DC-8 aircrafts for some days is illustrated in Figures 3 and 4. In general, the model captured the vertical variation patterns of the observed values for various species, with some exceptions. Noticeable among these are the consistent underpredictions for CO vertical profiles most of days. One of reasons for this under prediction is attributed to the inadequate representation of the transport of pollution associated with biomass burning from outside the domain (Mathur et al., 2005; McKeen et al., 2002). The significant underpredictions of CO during July 20 and July 22, 2005, further support this explanation as the aerosol index images from the TOMS satellite observations (<http://toms.gsfc.nasa.gov/>) clearly show that the eastern U.S. was significantly influenced by large forest fires in Alaska during these days. Another noticeable discrepancy is the consistent underpredictions of observed NO at altitudes greater than 3000 m (Figure 4). This may be because the aircraft and lightning NO emissions are not included in the current model emission inventory. The model had a good performance for HNO₃ most of time except on 7/9, 7/18 and 8/11. The modeled SO₂ concentrations

are generally higher than the observations at the low altitude (<200 m) but close to the observations at the high altitude relative to the P-3 measurements.

The model reproduced the vertical profiles of water vapor and wind speed very well most of time with slight over predictions of water vapor at low altitudes relative to P-3 observations (not shown). The model also tracked the vertical variations of temperatures, pressures and wind directions very well most of time (not shown).

3.3 Time-series comparison and diagnostic evaluation at the AIRMAP sites during the 2004 ICARTT

Figure 5 presents an example of time-series comparisons and scatter plots of the model predictions and observations for O₃, CO, NO, NO_y, SO₂, and JNO₂ (photolysis rates of NO₂) at the CS site. The model captured the hourly variations and broad synoptic changes seen in the observations of different gas species (O₃, NO₂, CO, NO_y, PAN) (correlation coefficient > 0.49, see Table 1) except NO and SO₂ at each site, although there were occasional major excursions. The model underpredicted CO by 20-50% consistently at each site, like those comparisons for the vertical profiles. The model reproduced the observed temperatures with ~±5% errors and relative humidity (RH) with ~±10% at each site very well but over predicted wind speed.

For the photolysis rates of NO₂, we focus our analysis on daytime data by excluding data where JNO₂ < 5 × 10⁻⁵ s⁻¹. Table 1 indicates that the model reproduced 49.6%, 43.1% and 53.8% of observed JNO₂ values within a factor of 1.5 at the CS, MWO and TF sites, respectively. DeMore et al. (1997) suggest that a ±20% uncertainty was associated with uncertainty in the cross-section and quantum yield data in the calculation of JNO₂ values. The sensitivity tests of Hanna et al. (2001) indicate that a 50% uncertainty in JNO₂ could cause about a 40 ppbv, or a 20% uncertainty in predicted maximum O₃ concentration in their cases. This suggests the need for more accurate determination of the JNO₂ values in the model to improve O₃ predictions.

The [O₃]/[NO_x] values can be used to determine NO_x-sensitive and VOC-sensitive chemical regimes. NO₂ concentrations were estimated on the basis of the NO/NO₂/O₃ photo-stationary steady state assumption. [O₃]/[NO_x] values > 46 indicate strong NO_x-sensitive conditions, whereas values < 14 indicate VOC-

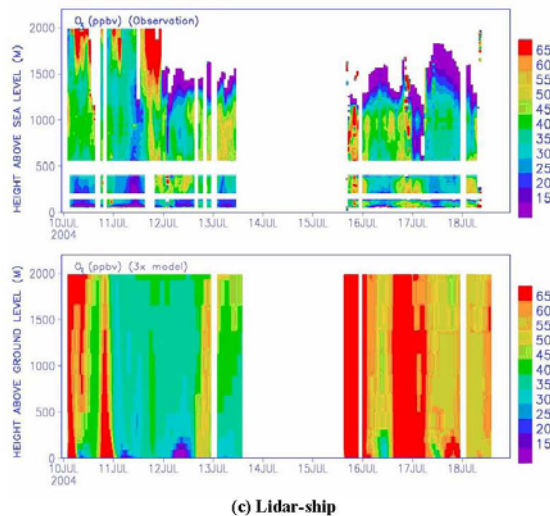
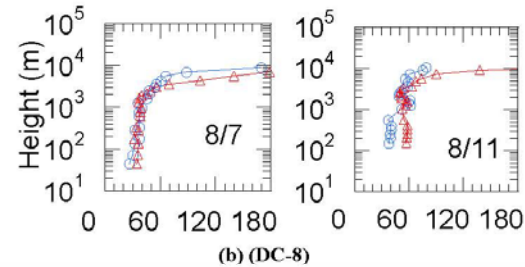
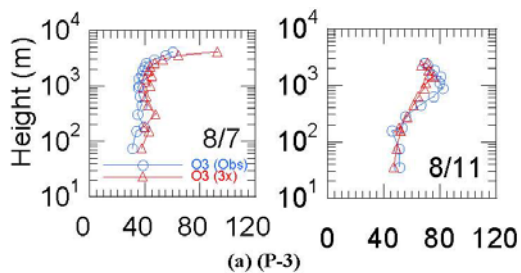


Fig. 2. Comparison of vertical O_3 (ppbv) profiles for the model and observations from (a) aircraft P-3, (b) aircraft DC-8 and (c) ship-Lidar during the ICARTT period. In (a) and (b), blue: observation and red: model.

sensitive conditions (Arnold et al., 2003). Table 2 summarizes the variations in the $[O_3]/[NO_x]$ ratio at the CS, WMO, and TF sites, revealing that for the most part, the model correctly reproduced the temporal variations in the observed $[O_3]/[NO_x]$ ratios across the different conditions represented at the three sites. Both model and observations show that the CS and MWO sites are mainly under strongly NO_x -sensitive conditions (>66%).

The upper limits of the ozone production efficiencies (ϵ_N) value can be estimated by the O_3 - NO_z slope. Following Arnold et al. (2003), both modeled and observed O_3 - NO_z slopes are obtained for only observational data with $[O_3]/[NO_x] > 46$ at the three sites. There is

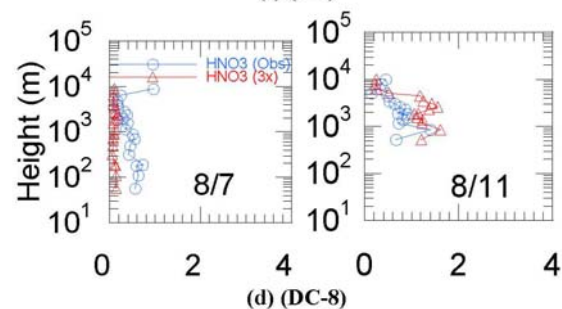
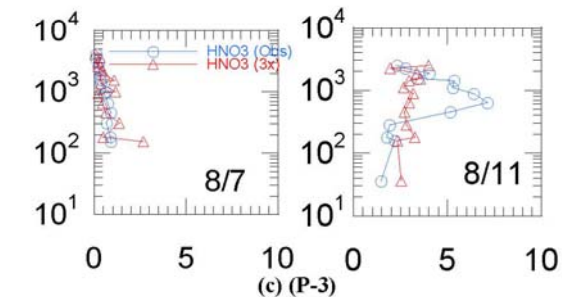
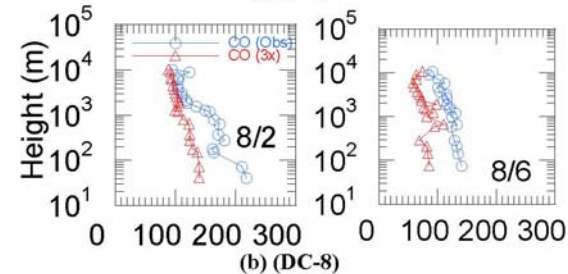
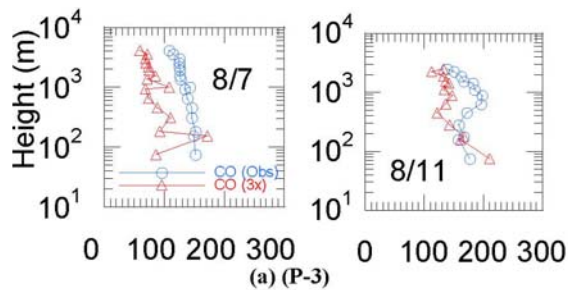


Fig. 3. Comparison of vertical CO and HNO_3 (ppbv) profiles for the models and observations from the aircrafts P-3 (a, c), and DC-8 (b, d) during the ICARTT period. Blue: observation and red: model.

significant correlation between O_3 and NO_z for both model predictions and observations ($r > 0.77$) at the three sites (see Fig. 6 and Table 3). Both modeled and observed values of ozone production efficiency at the three sites are in the estimated ranges (5 to 10) of other investigators (Olszyna et al., 1994) at rural sites in the eastern US, although the modeled values (5.2 to 6.7) are systematically lower than those of the observations (8.5 to 10.7).

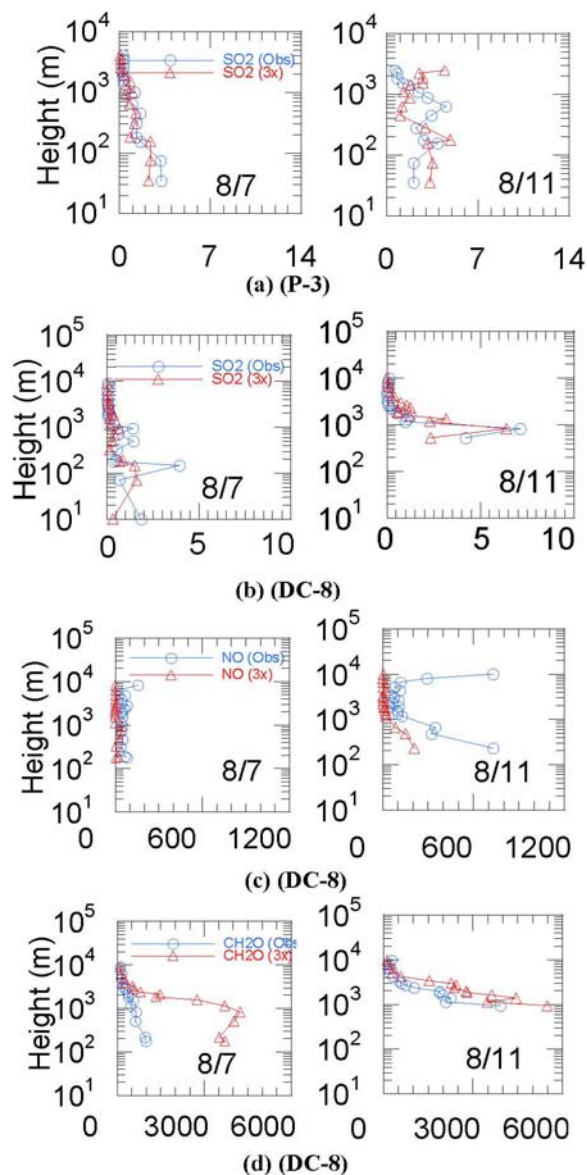


Fig. 4. The same as Figure 4 but for SO₂ (ppbv), NO (pptv) and HCHO (pptv). Blue: observation and red: model.

4. REFERENCES

Arnold, J.R., R.L. Dennis, and G.S. Tonnesen, 2003: Diagnostic evaluation of numerical air quality models with specialized ambient observations: testing the Community Multiscale Air Quality modeling system (CMAQ) at selected SOS 95 ground sites. *Atmospheric Environment*, 37, 1185-1198.

Byun, D.W. and J.K.S. Ching, Eds., 1999: Science algorithms of the EPA Models-3 Community Multi-scale Air Quality (CMAQ) modeling system, EPA/600/R-99/030, Office of

Table 1. Statistical summaries of the comparisons of the model results with the observations at the AIRMAP sites during the 2004 ICARTT.

Parameters	<C>*		r	% within a factor of 1.5**	% within a factor of 2**
	Obs	Model			
Castle Springs (N=1047)					
O ₃	35.17	43.63	0.493	66.6	90.1
NO	0.14	0.05	0.222	12.1	22.5
CO	188.84	108.78	0.706	19.3	74.7
NO _y	2.27	3.14	0.587	43.6	67.7
SO ₂	1.16	0.87	0.388	29.6	45.8
JNO ₂ (1/s)	3.18E-03	4.07E-03	0.820	49.6	63.4
Temperature (C)	19.65	19.78	0.867	100.0	100.0
RH (%)	78.69	71.64	0.781	97.7	100.0
Wind direction	182	198	0.455	63.0	78.6
Wind speed (m/s)	1.04	3.25	0.426	11.7	24.3
Isle of Schoals (N=1078)					
O ₃	36.68	52.31	0.541	56.9	80.2
CO	171.70	121.15	0.610	60.9	90.3
NO	0.76	0.18	0.448	0.8	3.5
Mount Washington (N=1076)					
O ₃	45.87	45.85	0.554	87.7	98.8
NO	3.64	0.01	-0.054	8.9	13.8
CO	152.43	95.19	0.301	46.7	84.3
NO _y	4.04	2.23	-0.060	26.6	38.4
SO ₂	0.74	0.30	-0.001	18.0	32.6
JNO ₂ (1/s)	3.59E-03	4.43E-03	0.768	43.1	61.9
Thompson Farm (N=1067)					
O ₃	28.80	41.68	0.751	48.1	73.6
NO	0.33	0.29	0.436	31.3	51.3
CO	173.07	154.66	0.593	77.7	98.5
NO _y	3.93	7.26	0.321	28.8	51.6
SO ₂	1.22	1.63	0.084	14.3	25.3
JNO ₂ (1/s)	3.19E-03	3.90E-03	0.865	53.8	68.1
Temperature (C)	20.33	20.44	0.887	99.9	100.0
RH (%)	80.97	75.18	0.829	98.5	100.0
Wind direction	198	177	0.530	73.2	83.7
Wind speed (m/s)	0.96	3.29	0.462	8.0	16.8

* <C> is the mean concentration (ppb)

** Percentages (%) are the percentages of the comparison points at which model results are within a factor of 1.5 and 2 of the observations. N is number of samples.

Table 2. Statistical summary of number of hours for response surface indicator ratios (O₃/NO_x) for model and observations at each site during the period of July 1 to August 15, 2004. The values in parentheses are the percentages (%).

O ₃ /NO _x	Castle Springs		Mount Washington		Thompson Farm	
	Obs	Model	Obs	Model	Obs	Model
0-14	32 (7)	18 (4)	13 (4)	0 (0)	181 (38)	105 (22)
15-25	34 (7)	19 (4)	3 (1)	0 (0)	51 (11)	72 (15)
26-45	94 (20)	18 (4)	16 (5)	2 (1)	59 (12)	125 (26)
>46	312 (66)	417 (88)	285 (90)	315 (99)	188 (39)	177 (37)
Total hours	472 (100)	472 (100)	317 (100)	317 (100)	479 (100)	479 (100)

Table 3. Correlations between O₃ and NO₂ for the NO_x-limited conditions indicated by the observational data with [O₃]/[NO_x] > 46 (aged air masses) at the CS, WMO and TF sites during the period of July 1 to August 15, 2004. N is number of points and r is correlation coefficient.

Sites	Regression equations
Castle Springs (N=312)	Obs: [O ₃] = 10.7[NO ₂] + 22.8, r ² = 0.703
	Model: [O ₃] = 6.4[NO ₂] + 30.1, r ² = 0.614
Mount Washington (N=285)	Obs: [O ₃] = 9.5[NO ₂] + 41.5, r ² = 0.181
	Model: [O ₃] = 6.7[NO ₂] + 32.4, r ² = 0.616
Thompson Farm (N=188)	Obs: [O ₃] = 8.5[NO ₂] + 26.4, r ² = 0.803
	Model: [O ₃] = 5.2[NO ₂] + 34.0, r ² = 0.831

Research and Development, U.S. Environmental Protection Agency.

DeMore, W.B., S.P. Sander, C.J. Howard, A.R. Ravishankara, D.M. Golden, C.E. Kolb, R.F. Hampson, M.J. Kurylo, and M.J. Molina, 1997: Chemical kinetics and photochemical data for use in stratospheric modeling, Eval. 12, NASA Jet

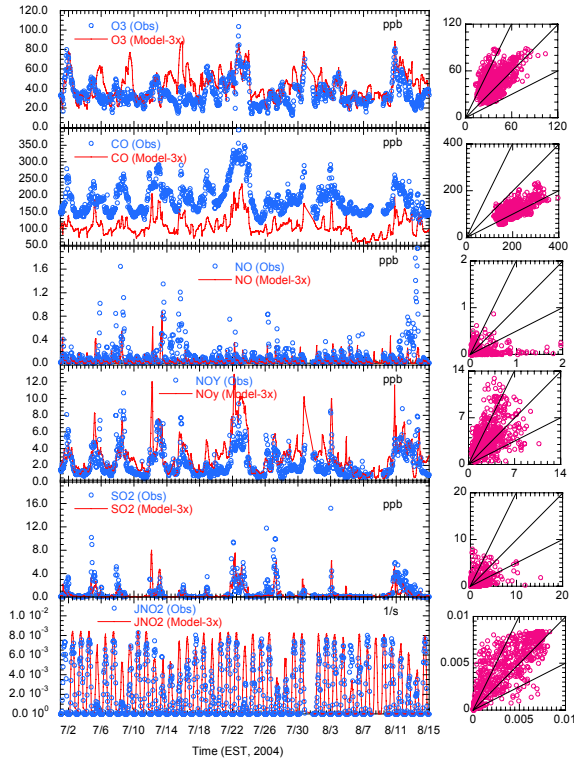


Fig. 5. Time-series and scatter plots of model predictions and observations for each parameter at the Castle Springs site.

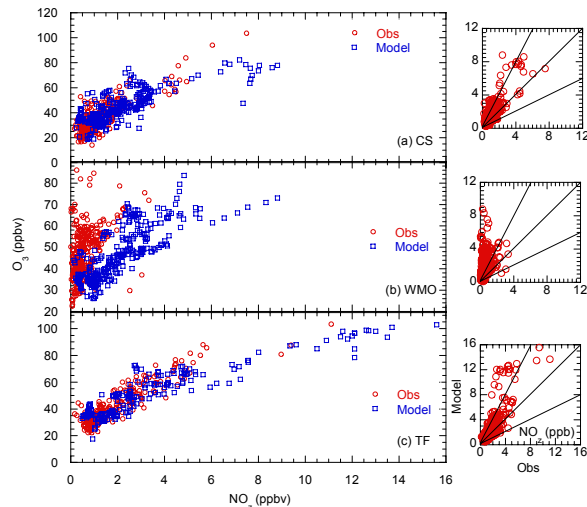


Fig. 6. O_3 as a function of NO_z for the NO_x -limited conditions indicated by the observational data with $[O_3]/[NO_x] > 46$ at (a) CS, (b) WMO, and (c) HF. Right panels are scatter plots of modeled and observed NO_z (ppbv).

Propul. Lab., Calif. Inst. Of Technol., Pasadena.
Hanna, S.R., Z. Lu, H.C. Frey, N. Wheeler, J.

Vukovich, S. Arunachalam, M. Fernau, and D.A.Hansen, 2001: Uncertainties in predicted ozone concentrations due to input uncertainties for the UAM-V photochemical grid model applied to the July 1995 OTAG domain. *Atmospheric Environment*, 35, 891-903.

Mathur et. al., 2004. Adaptation and application of the Community Multiscale Air Quality (CMAQ) modeling system for real-time air quality forecasting during the summer of 2004, Proc. 2004 Models-3 Conference, October 18-20, 2004,

Mathur, R., et al., 2005. Multiscale air quality simulation platform (MAQSIP): Initial applications and performance for tropospheric ozone and particulate matter, *Journal of Geophysical Research*, 110, D13308, doi:10.1029/2004JD004918.

Mckeen, S.A., et al., 2002. Ozone production from Canadian wildfires during June and July of 1995, *Journal of Geophysical Research*, 107(D14), 4192, doi:10.1029/2001JD000697.

Olszyna, K.J., E.M. Bailey, R. Simonaitis, and J.F. Meagher, 1994: O_3 and NO_y relationships at a rural site. *Journal of Geophysical Research*, 99, 14,557-14,563.

Otte, T.L., et al., 2005. Linking the Eta model with the community multiscale air quality (CMAQ) modeling system to build a national air quality forecasting system. *Weather and Forecasting*, 20, 367-384, 2005.

Pouliot, G.A., 2005. The emissions processing system for the Eta/CMAQ air quality forecast system, Proc. 7th Conf. on Atmospheric Chemistry, The 85th AMS Annual Meeting, Paper 4.5, Amer. Meteor. Soc., San Diego, CA.

Rogers, E., T. Black, D. Deaven, G. DiMego, Q. Zhao, M. Baldwin, N. Junker, and Y. Lin. 1996: Changes to the operational "early" Eta Analysis/Forecast System at the National Centers for Environmental Prediction. *Wea. Forecasting*, 11, 391-413.

U.S. EPA, 1991. Guideline for regulatory application of the urban airshed model. USEPA Report No. EPA-450/4-91-013. U.S. EPA, Office of Air Quality Planning and Standards, Research Triangle Park, North Carolina.

Disclaimer The research presented here was performed under the Memorandum of Understanding between the U.S. Environmental Protection Agency (EPA) and the U.S. Department of Commerce's National Oceanic and Atmospheric Administration (NOAA) and under agreement number DW13921548. This work constitutes a contribution to the NOAA Air Quality Program. Although it has been reviewed by EPA and NOAA and approved for publication, it does not necessarily reflect their policies or views.